

High performance thin-film lithium niobate MZ modulator ready for massive production

Heng Li¹, Qunan Chen², Ye Liu¹, Yongqian Tang¹, Qiaoyin Lu¹, Mingzhi Lu², and Weihua Guo^{1,2}

¹Wuhan National Laboratory for Optoelectronics, Huazhong University of Science and Technology, Wuhan, China

²Ningbo Ori-chip Optoelectronics Technology LTD, Ningbo, China
guow@hust.edu.cn

Abstract: Through photolithography we fabricated high-performance thin-film lithium niobate modulators on full 4-inch wafers with low $V_{\pi}L$, wide bandwidth and low insertion loss. The waveguide loss is one of the lowest among similar work. © 2022 The Author(s)

1. Introduction

As typical external modulators, InP and silicon Mach-Zehnder (MZ) modulators can achieve ultra-high bandwidth and are now widely used in long-haul communications. Silicon MZ modulators are expanding their usage quickly in data centers as well. However, both types of modulators are also facing their own challenges such as: InP MZ modulators need temperature control and are quite expensive; silicon MZ modulators suffer from high insertion loss and bandwidth limitation. Traditional lithium niobate modulators have large size due to the weak optical confinement. Recently a new type of platform-thin-film lithium niobate (TFLN)-for high speed MZ modulators have attracted lots of attention due to their intrinsic high bandwidth and low loss. High performance demos have been achieved by different groups all over the world. But to really make this type of modulators widely deployable, processing suitable for massive production has to be established, e.g. full wafer processing based on photolithography has to be realized. In [8], great progress has been achieved where low loss waveguides have been demonstrated based on photolithography on full 4(6)-inch wafers. However, as far as we know fabrication of high performance MZ modulators based on full wafer processing through photolithography at a commercial fab has not been reported yet.

In this work, we demonstrated a MZ modulator fabricated based on photolithography, instead of e-beam lithography as most publications showed, on full 4-inch TFLN wafers at a commercial fab. Good performance has been demonstrated including $V_{\pi}L$ of $1.98 \text{ V}\cdot\text{cm}$, wide modulation bandwidth ($> 67 \text{ GHz}$) and low insertion loss (2.5 dB). This is an important step forward toward massive production of TFLN high speed MZ modulators.

2. Device structure

The modulator was fabricated on full 4-inch x-cut TFLN wafer with high impedance silicon substrate. Figure 1 shows microscope image of the MZ modulator which includes two 2×2 multi-mode interferometer (MMI) splitters, spot-size converters (SSC) at the input and output ports, single drive coplanar wave (CPW) traveling-wave electrode for push-pull modulation, the input and output GSG pads for RF signal input and output, thermal phase shifters on each arm of the modulator for DC bias.

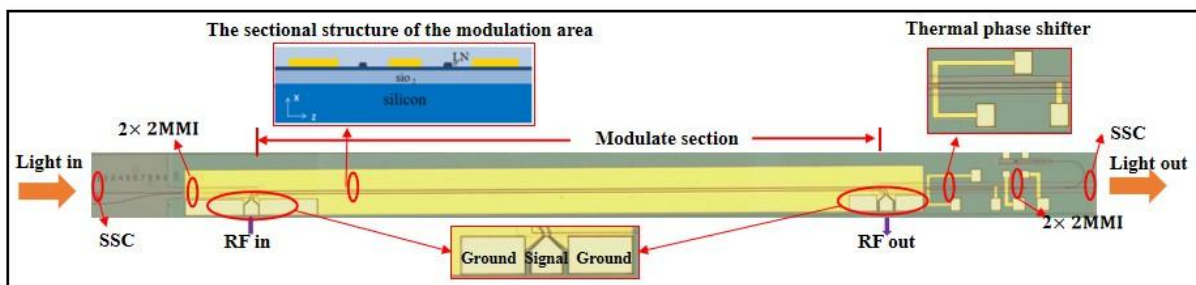


Fig. 1. The schematic of the MZ modulator.

3. Device characterization

The device is fabricated on Ori-Chip's dedicated TFLN fab in a production manner. Total of 720 devices were fabricated on a single 4-inch wafer. High quality etching is a big challenge for the TFLN platform especially when photolithography patterning has been used. After careful optimizing the photolithography process and the ICP dry etching process, we have achieved waveguides with straight and smooth sidewalls across the whole 4-inch wafer. The SEM image is shown in Fig. 2(a). To evaluate the waveguide propagation loss, waveguides with different lengths were fabricated as seen by the inset of Fig. 2(b). The insertion loss of these waveguides was measured by

coupling through fiber pigtails with suitable mode field diameter (MFD). Loss versus the waveguide length increase is shown in Fig. 2(b), from which the waveguide propagation loss of 0.23 dB/cm is extrapolated.

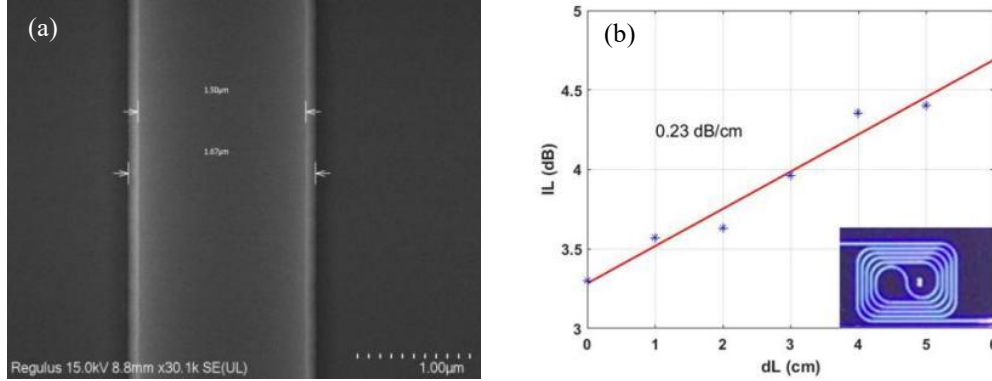


Fig. 2 (a) SEM image of the etched TFLN waveguide; (b) loss of the TFLN waveguides (The inset shows the microscope image of one of the test structures.).

Table 1 shows recent works on TFLN waveguide loss. Most of the researches choose EBL for waveguide patterning. Compared with EBL, photolithography has much higher efficiency and is suitable for massive production. Clearly our loss is one of the best results of similar work. The insertion loss of the whole modulator is around 2.5 dB, of which 0.2 dB is from the MMIs, 0.3 dB is from the waveguide and 2 dB is from the fiber coupling (two facets).

Table 1. Loss comparison of TFLN waveguides

Loss (dB)	Pattern definition	Waveguide width(μm)	λ (μm)	Ref
0.4	EBL	1	1.55	[1]
0.027	EBL	2.4	1.59	[2]
3	EBL	0.9	1.55	[3]
0.37	EBL	2	1.55	[4]
0.77	EBL	1	1.55	[4]
0.62	EBL	1.8	1.542	[5]
0.15	EBL	4	1.55	[6]
0.3	EBL	1	1.55	[6]
4.18 \pm 0.7	Photolithography	2	1.55	[7]
0.27	Photolithography	2	1.59-1.6	[8]
0.7	Photolithography	1.5	1.55	[9]
0.23	Photolithography	1.5	1.55	our work

To measure V_{π} , a 1 kHz triangle wave with 5.5 V V_{PP} was applied on the travelling-wave electrode and a photodetector is used to monitor the power of the output light. The oscilloscope traces of the modulation wave and the PD detected output signal are shown in Fig.3(a), from which V_{π} is determined to be 2.64 V. Based on the 7500- μm electrode length, $V_{\pi}L$ is determined to be 1.98 V \cdot cm, which is slightly higher than our previous result [9]. The modulator also integrates thermal phase shifters on both arms. By apply thermal power onto the thermal phase shifter, a response curve of the modulator is obtained as shown in Fig.3(b), from which it can be seen that a π -phase shift power of 45 mW is obtained and the extinction ratio is close to 35 dB.

A 67-GHz vector network analyzer (VNA) is used to measure the EO-response of the modulator. Figure 3(c) shows the EO-response curve and the S11. In the figure, we can see that limited by the 67 GHz measuring range, the 3 dB bandwidth is at least 67 GHz, and from S11 parameter we can see that the return loss of the microwave electrical signal is below -20dB almost across the whole spectrum. The modulator is also used as an intensity modulator to transmit the PAM-4 signal at 53 GBaud. The back-to-back eye-diagram is shown in Fig. 3(d) with clear eye opening and the extinction ratio is 5.28 dB. TDECQ is measured to be 1.26 dB.

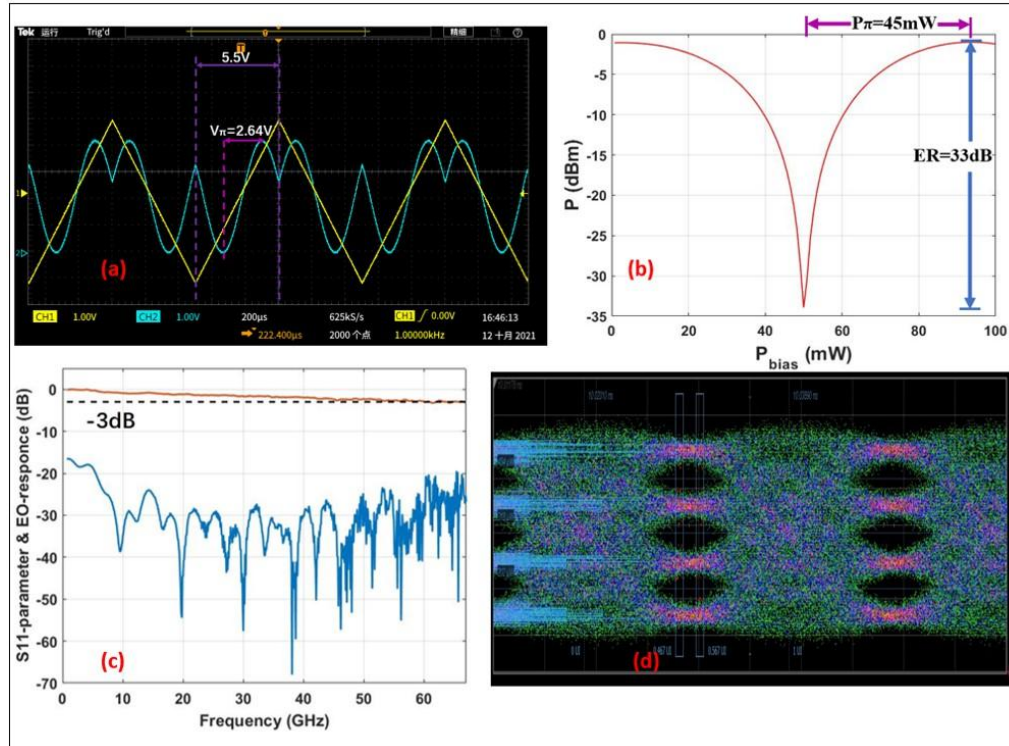


Fig. 3.(a) Schematic diagram of V_{π} measurement (the yellow line is the triangular signal applied on the modulator, and the blue line is the modulated optical signal intensity); (b) transmission as a function of thermal phase shifter's bias power; (c) the EO-response and S_{11} of the TFLN modulator; (d) measured PAM-4 modulation optical eye diagrams at 53 GBaud.

4. Conclusion

In this work, high-performance TFLN modulators were fabricated at Ori-Chip's TFLN fab on full 4-inch TFLN wafers. By using photolithography for waveguide definition, low $V_{\pi}L$ ($1.98 \text{ V} \cdot \text{cm}$), wide modulation bandwidth ($> 67 \text{ GHz}$) and low insertion loss (2.5 dB, on-chip loss about 0.5 dB) was obtained. The optical PAM-4 eye-diagrams at 53 Gbaud with measured extinction ratio of 5.28 dB. Thermal phase shifters' π -phase shift power is 45 mW with the extinction ratio close to 35 dB and the waveguide loss (0.23 dB/cm) is the lowest among similar work.

5. Funding

This work was supported by the National Key Research and Development Program of China (2019YFB2203304).

6. References

- [1] Inna Krasnokutskaya, Jean-Luc J. Tambasco, Xijun Li, and Alberto Peruzzo, "Ultra-low loss photonic circuits in lithium niobate on insulator," *Opt. Express* 26, 897-904 (2018).
- [2] Mian Zhang, Cheng Wang, Rebecca Cheng, Amirhassan Shams-Ansari, and Marko Lončar, "Monolithic ultra-high-Q lithium niobate microring resonator," *Optica* 4, 1536-1537 (2017).
- [3] Cheng Wang, Mian Zhang, Brian Stern, Michal Lipson, and Marko Lončar, "Nanophotonic lithium niobate electro-optic modulators," *Opt. Express* 26, 1547-1555 (2018).
- [4] Lutong Cai, Ashraf Mahmoud, and Gianluca Piazza, "Low-loss waveguides on Y-cut thin film lithium niobate: towards acousto-optic applications," *Opt. Express* 27, 9794-9802 (2019).
- [5] Jingwei Ling, Yang He, Rui Luo, Mingxiao Li, Hanxiao Liang, and Qiang Lin, "Athermal lithium niobate microresonator," *Opt. Express* 28, 21682-21691 (2020).
- [6] Mengyue Xu, Mingbo He, Hongguang Zhang, Jian Jian, Ying Pan, Xiaoyue Liu, Lifeng Chen, Xiangyu Meng, Hui Chen, Zhaohui Li, Xi Xiao, Shaohua Yu, Siyuan Yu and Xinlun Cai. "High-performance coherent optical modulators based on thin-film lithium niobate platform." *Nature Communications* 11 (2020): n. pag.
- [7] M. Prost, G. Liu, and S. J. Ben Yoo, "A Compact Thin-Film Lithium Niobate Platform with Arrayed Waveguide Gratings and MMIs," in *Optical Fiber Communication Conference, OSA Technical Digest* (online) (Optical Society of America, 2018), paper Tu3A.3.
- [8] Kevin Luke, Prashanta Kharel, Christian Reimer, Lingyan He, Marko Loncar, and Mian Zhang, "Wafer-scale low-loss lithium niobate photonic integrated circuits," *Opt. Express* 28, 24452-24458 (2020).
- [9] H. Li, Y. Liu, J. Liu, S. Tan, Q. Lu, M. Lu, and W. Guo, "Low V_{π} silicon-based x-cut thin-film lithium niobate MZ modulators fabricated by photolithography," in *Asia Communications and Photonics Conference/International Conference on Information Photonics and Optical Communications 2020 (ACP/IPOC)*, K. Xu, D. Simeonidou, C. Chang-Hasnain, N. Wada, X. Ren, Z. Zhukov, P. Perry Shum, Y. Ji, J. Zhang, X. Zhou, C. Lu, and L. Wosinska, eds., *OSA Technical Digest* (Optical Society of America, 2020), paper S4D.4.